Corrigendum

The substrate as a skeleton: ground reaction forces from a soft-bodied legged animal

Huai-Ti Lin and Barry A. Trimmer

10.1242/jeb.060566

There was an error published in *J. Exp. Biol.* **213**, 1133-1142.

In the original Fig. 5, the scale bar for the fore–aft ground reaction force (fGRF) should be 0.3 body weight (as for the normal ground reaction force). The reaction force in the fore–aft direction is therefore on the same scale as in the vertical direction. In the figure legend, the following sentences should consequently be removed: 'Note that fGRF (scale bar is 5 BW) is much larger than nGRF (scale bar 0.3 BW).' and 'A Manduca fifth instar caterpillar covered 33–45% of body length in each crawl.'

This error affects three places in the text but does not change the conclusions or overall message of this paper.

On p. 1138, Results, 'Prolegs fore-aft loading', the first sentence should read: 'The reaction forces in the direction of locomotion (fGRF) are similar in magnitude to the normal loads despite the lack of body dynamics (Fig. 5A).'

On p. 1139, Discussion, 'Stiff legs push, soft legs pull', the last sentence should read: 'Although the nGRFs during horizontal crawling are positive and therefore compress the prolegs (weight-bearing), these forces are fractions of body weight and can be easily supported by baseline body pressure.'

On p. 1140, Discussion, 'Antagonist stretching and efficiency', the sentence should read: 'Forces in the axial direction are responsible for extending the body and restoring muscle length.'

In addition, in Eqns 1 and 3, we only work with the magnitude of acceleration and force. The correct versions of the equations are presented below.

$$\left|\mathbf{a}\right| = \frac{d}{t^2} = \frac{8.52(\mathrm{mm})}{1.817^2(\mathrm{s}^2)} = 2.58\left(\frac{\mathrm{mm}}{\mathrm{s}^2}\right) \quad (1)$$

$$\left|\mathbf{F}\right| = m\left|\mathbf{a}\right| = 2.5(\mathrm{g}) \times 0.3(\mathrm{BW}) \times 2.58\left(\frac{\mathrm{mm}}{\mathrm{s}^2}\right) = 1.94(\mu\mathrm{N}) \quad (2)$$

The authors apologize to readers for these errors.

The Journal of Experimental Biology 213, 1133-1142

doi:10.1242/jeb.037796

The substrate as a skeleton: ground reaction forces from a soft-bodied legged animal

Huai-Ti Lin* and Barry A. Trimmer
Tufts University, 165 Packard Avenue, Medford, MA, USA
*Author for correspondence (huai-ti.lin@tufts.edu)

Accepted 9 December 2009

SUMMARY

The measurement of forces generated during locomotion is essential for the development of accurate mechanical models of animal movements. However, animals that lack a stiff skeleton tend to dissipate locomotor forces in large tissue deformation and most have complex or poorly defined substrate contacts. Under these conditions, measuring propulsive and supportive forces is very difficult. One group that is an exception to this problem is lepidopteran larvae which, despite lacking a rigid skeleton, have well-developed limbs (the prolegs) that can be used for climbing in complex branched structures and on a variety of surfaces. Caterpillars therefore are excellent for examining the relationship between soft body deformation and substrate reaction forces during locomotion. In this study, we devised a method to measure the ground reaction forces (GRFs) at multiple contact points during crawling by the tobacco hornworm (*Manduca sexta*). Most abdominal prolegs bear similar body weight during their stance phase. Interestingly, forward reaction forces did not come from pushing off the substrate. Instead, most positive reaction forces came from anterior abdominal prolegs loaded in tension while posterior legs produced drag in most instances. The counteracting GRFs effectively stretch the animal axially during the second stage of a crawl cycle. These findings help in understanding how a terrestrial soft-bodied animal can interact with its substrate to control deformation without hydraulic actuation. The results also provide insights into the behavioral and mechanistic constraints leading to the evolution of diverse proleg arrangements in different species of caterpillar.

Key words: GRFs, legged locomotion, soft-bodied animal, *Manduca sexta*, caterpillar.

INTRODUCTION

Locomotion by soft-bodied animals

Articulated (stiff, jointed) and hydrostatic (soft wall, pressurized) skeletons (Chapman, 1958) are the two primary structural models used to characterize and explain the biomechanics of animal locomotion. In an articulated system, movements can be described precisely by the center of mass position and joint angles (Colobert et al., 2006; Holmes et al., 2006). Muscles work antagonistically around a joint to produce directionally constrained motions and structural levers allow the mechanical exchange of force and displacement.

A similar process occurs in many soft-bodied animals that exploit incompressible body-fluid to transmit forces and to actuate body parts (Kier, 1992; Niebur and Erdos, 1991; Quillin, 1998; Skierczynski et al., 1996; Wadepuhl and Beyn, 1989). For example, most annelids use circumferential muscles that operate antagonistically with longitudinal muscles to control extension and shortening (Kristan et al., 2005; Quillin, 1999). These animals produce different postures using a temporary stiff hydrostatic skeleton. Even animals such as the octopus, which does not have an open fluid-filled cavity, use the viscous, semi-fluid properties of connective tissues and muscles to control movements (muscular hydrostats) (Kier and Stella, 2007).

Most current models of hydrostatic skeletons make the general assumption of volume conservation and use geometric approaches to predict movements (Skierczynski et al., 1996; Smolianinov and Mazurov, 1976; Wadepuhl and Beyn, 1989), sometimes employing tissue material properties in the simulations (Chiel et al., 1992; Herrel et al., 2002; Kier and Smith, 1985; Nishikawa et al., 1999). Although these modeling approaches can be used to estimate mechanical interactions, direct measurements of locomotor forces by soft-bodied animals remain scarce, and highly constrained by technical limitations (Keudel and Schrader, 1999; McKenzie and Dexter, 1988a; McKenzie and Dexter, 1988b; Quillin, 2000).

Caterpillars as a model system

One group of animals that makes an attractive model system for studying such locomotor forces is the larval stage of the Lepidoptera (i.e. caterpillars) because most caterpillars interact with the environment *via* discrete contacts (prolegs). By measuring the substrate reaction forces of each proleg simultaneously, it should be possible to determine how body deformation translates into locomotor dynamics. Caterpillars are also interesting from biomechanical and neurobiological perspectives because they are pressurized soft cylinders capable of climbing in complex three-dimensional environments. This is accomplished with only longitudinal muscles and a few short oblique muscles, making it puzzling how they manage to co-ordinate shortening and extension using a non-septate fluid and tissue-filled body cavity.

Caterpillars usually employ the abdominal prolegs for attachment to the substrate and produce anterograde waves of movement, but there is considerable species diversity in the arrangement of these appendages and in their use during locomotion (Miller et al., 2006; Snodgrass, 1993). Four pairs of abdominal prolegs (on abdominal segments 3 to 6; A3–A6) and a pair of terminal (anal) prolegs (on abdominal segment 10; TP) are thought to be the ancestral and/or dominant form for lepidopteron (as labeled in Fig. 2) (Forbes, 1910; Hinton, 1955) but prolegs in different species can be lost from any segment (Wagner, 2005). For example, most caterpillars in the family *Notodontidae* have modified terminal prolegs for purposes

other than locomotion and in the family *Noctuidae* both anterior and posterior prolegs are reduced. The subfamily *Hypeninae* have lost functional A3 prolegs while the terminal prolegs are elongated, and members of the subfamily *Catocalinae* have even lost the A4 prolegs. Species such as *Parallelia bistriaris* (maple looper) and *Caenurgina crassiuscula* (clover looper) do not have prolegs on segments A3 or A4 and they move with looping gaits. Members of the subfamily *Plusiinae* (cabbage looper, soybeam looper, celery looper) move by 'inching' with prolegs on A5, A6, and the terminal segments. Of course, the inchworms (*Geometridae*) all perform inching locomotion with only the A6 and terminal prolegs. Some lepidopteran larvae do not need prolegs for locomotion and have reduced them into a continuous ventrum (slug caterpillars) (Epstein, 1996; Rubinoff and Haines, 2005) or transformed posterior legs into a hydraulic warning display (family *Notodontidae*). Case-bearer caterpillars only employ the six thoracic legs for locomotion. On top of this diversity, there is a large range of body size and cuticular adornments across lepidopteran species (Miller et al., 2006). It is therefore very important to recognize the body morphology and modes of locomotion. In this study, we only focused on large caterpillars with the ancestral body plan such as *Manduca*, which might inform us about some general strategies for locomotory movements.

Manduca locomotion and mechanics

The tobacco hornworm (*Manduca sexta* L.) is a well-studied model system in neurobiology, physiology and ecology. Because their muscle anatomy is known so well (Barth, 1937; Eaton, 1988; Kopec, 1919; Libby, 1959; Snodgrass, 1961; Snodgrass, 1993) and each muscle is generally innervated by a single motoneuron (Levine and Truman, 1985; Taylor and Truman, 1974; Weeks and Truman, 1984) these caterpillars show great promise for electromyographic studies of soft-bodied locomotion (Belanger and Trimmer, 2000; Dominick and Truman, 1986; Johnston and Levine, 1996a; Johnston and Levine, 1996b; Mezoff et al., 2004; Simon and Trimmer, 2009). *Manduca* is a relatively large insect (which helps force measurements) using four pairs of abdominal prolegs and a pair of terminal prolegs to generate most of its motion. A crawl typically consists of anterograde waves of body muscle contractions with the prolegs releasing their grip (Belanger et al., 2000; Mezoff et al., 2004) to be carried forward for re-attachment. Several segments are in swing phase simultaneously and the wave of motion usually continues into the thorax and head as the next cycle begins from the terminal prolegs (Trimmer and Issberner, 2007). *Manduca* caterpillars weighing 2 g move at an average speed of $3.10\pm0.24\,mm\,s^{-1}$ during horizontal locomotion with low acceleration and hence very small center of mass dynamics (van Griethuijsen and Trimmer, 2009).

In preliminary experiments it was found that *Manduca* are able to crawl horizontally even when the thoracic legs are removed. Apart from the unsupported thorax sliding across the substrate and slower movements, these crawls appeared normal with appropriately sequenced steps in the abdomen. Another interesting finding is that the hemocoele pressure of restrained (Mezoff et al., 2004) and crawling *Manduca* (H.T.L., unpublished data) is not isobarometric nor do the fluid pressure changes correlate well with movements. This is supported by phase-contrast synchrotron X-ray videography showing that internal tissues such as the gut, hemolymph and trachea are in constant motion (M. A. Simon, personal communication), presumably generating, and responding to, pressure gradients. During crawling, the gut movements in particular are quite large; this means we should be very careful interpreting static loads from inertial forces. In addition, the internal air cavity constitutes between 3 and 10% of body volume and air can be expelled during underwater locomotion, suggesting that the internal volume is not necessarily constant (H.T.L., unpublished preliminary data).

These prior observations suggest that caterpillar locomotion is biomechanically distinct from the current models of soft-bodied terrestrial crawling. In this study, the central questions we wanted to address were: (1) during crawling, how does a caterpillar extend its body without circumferential muscles?; (2) within a crawl cycle, how much weight shift occurs, and what are the roles of different prolegs?; (3) given that the body is not necessarily incompressible, how does *Manduca* transmit forces for posture support and propulsion?

A major finding is that caterpillars use the substrate to transmit forces from each contact point to other parts of the body. Instead of contact points propelling the center of mass forward, we propose that soft animals can employ an 'environmental skeleton'. In this view, posture generated by stiff hydrostatic control has a smaller secondary role in locomotion.

MATERIALS AND METHODS

The measurement challenge

Reaction forces are usually measured with a force plate larger than the animal's total contact area (Goldman et al., 2006; Heglund, 1981; Zumwalt et al., 2006) but *Manduca* moves so slowly that it exerts very weak inertial forces (forces associated with acceleration). In other words, the overall acceleration of the caterpillar does not adequately reflect the size or direction of local ground reaction forces, some of which cancel out when measured collectively. Furthermore, because caterpillars' bodies deform massively between contacts it is not desirable to measure forces on one leg at a time as can be done for animals with stiffer skeletons (Blickhan et al., 2007; Dutto et al., 2004; Roberts and Belliveau, 2005). Instead, reaction forces from each proleg should be measured independently and simultaneously. Recent breakthrough in developing micro force sensor units has made insect locomotor dynamics much more accessible (Bartsch et al., 2007; Lemmerhirt et al., 2006; Reinhardt et al., 2009). However, these microelectromechanical fabricated or precision-machined sensors are very expensive and require specialized maintenance. For our application, we constructed a robust, low cost, sensory array to resolve forces from each contact point simultaneously. Our observations of *Manduca* with amputated thoracic legs suggested that the prolegs are sufficient for crawling. Therefore, the number and spacing of sensors was arranged to optimally capture data from the prolegs. Reaction forces from the thoracic legs can occasionally be resolved with this array (usually a single combined thoracic force, rarely as separate segments) so they are reported where available. The sensor array was paved over most of the caterpillar length so that the center of mass and weight redistribution could be tracked during locomotion.

The *Manduca* force beam array

The device consisted of an array of cantilevered strain-gage based force beams each with four sensors arranged to detect both normal forces (i.e. perpendicular to the crawl, aligned with gravity in horizontal crawling; nGRF) and axial forces (i.e. fore–aft forces along the axis of a crawl; fGRF; Fig. 1A). The beams were arranged with a pitch of 3.81 mm per sensor, which is less than half the caterpillar average stride length (8.52±0.22 mm) (van Griethuijsen and Trimmer, 2009). Preliminary data showed that each pair of prolegs takes up to one-third of the body weight (<7 mN for a 2 g fifth instar) and three times the body weight in the fore–aft direction (<60 mN). A custom built control system provided AC excitation, analog amplification and

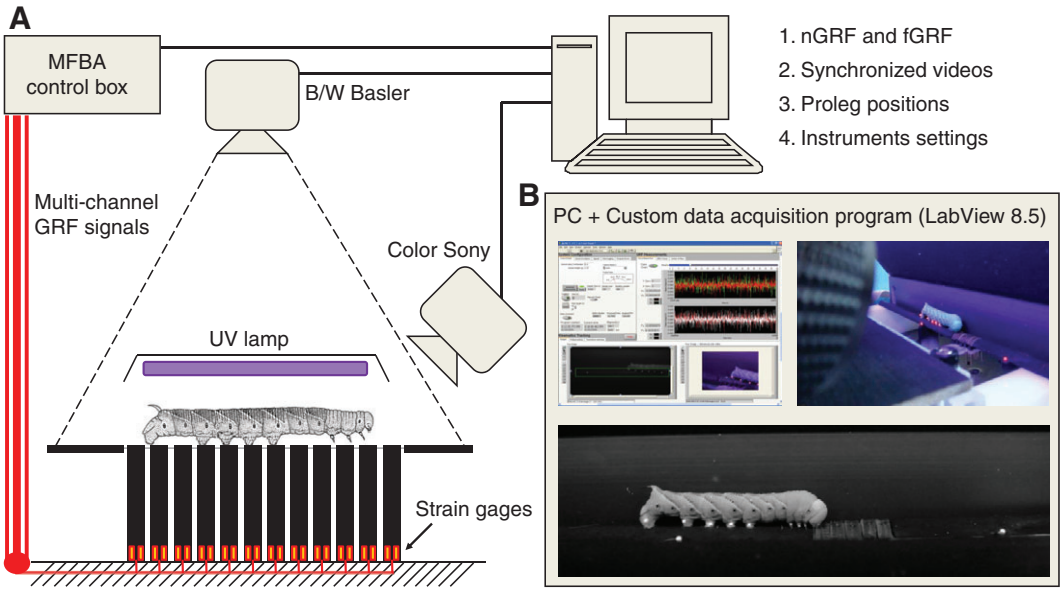

Fig. 1. *Manduca* force beam array (MFBA) setup. (A) Cantilever force beam with strain gages. Each force beam has strain gages bonded at its base to quantify deflection forces due to caterpillar steps. Force signals were passed through a control box for basic signal processing before going into the PC *via* a NI data acquisition card. (B) Proleg tracking and data acquisition. Caterpillars were marked with UV-black-paint-coated beads for video tracking. The image from a monochrome video camera was used to track the proleg markers and to calibrate their position relative to two fixed dots on the substrate. An additional color CCD camera recorded a close-up view to determine which legs were in contact with each beam. A custom LabView program acquired both the visual and force data after some hardware signal processing. The software further processed the data to output a set of data files.

basic signal processing. A Basler 206A high speed camera (Basler, Ahrensburg, Germany) was used for real-time two-dimensional (2-D) kinematics tracking and a Sony SSC S20 color camera (SONY, Tokyo, Japan) for detailed behavioral observation. Data collection was controlled by a custom program running in LabView 8.5 (National Instrument, Austin, TX, USA; Fig. 1B). The program took images from the kinematics camera and identified markers on the animal, transformed the coordinates according to the location of the substrate and marked the touchdown of prolegs in a force data spreadsheet. The GRF data were displayed in real-time to help monitor experimental progress. The program saved five data files for every experiment. This included a reference recording for noise and offset analysis, the raw force data, kinematics raw data, processed force data with kinematics markings, and the synchronized behavioral video. Because this device is unique and suitable for use with a variety of species it will be described in more technical detail in a separate publication.

Animal subjects

Healthy second day fifth instar *Manduca* sexta caterpillars were collected from our colony, with a body mass of between 1.5 and 3 g, corresponding to body length between 26.5 mm and 45.3 mm (based on a body dimension statistics for our colony, N=25). All animals were reared on an artificial diet and kept in a 17 h:7 h L:D cycle at 27°C. The colony maintenance and rearing protocol were as described by Bell and Joachim (Bell and Joachim, 1976). Animal subjects were weighed, sexed, and labeled before being placed in a large transparent container (conditioning chamber) for 20 min of free roaming. Eight animals were used in this study.

GRF recording procedure

During the development of the sensor device data was collected from two sets of beam arrays. A 1-D array consisting of 12 unidirectional force beams was use to collect weight shift information (range=45.72 mm, or ~100% resting length of a fifth instar *Manduca*). A second array consisting of five two degrees of freedom (2-D) force beams (range=19.05 mm, or ~40% resting length) was used for force correlation analysis. Prolegs were tracked using a bead (0.50±0.05 mm diameter) coated with clear red UV fluorescent paint (Risk Reactor, Dallas, OR, USA) placed on each proleg on one side of the animal (Fig. 1B). The wet paint allowed the red fluorescent beads to adhere to the proleg cuticle. A Black-Ray BL-15 UV lamp (UVP Inc., San Gabriel, CA, USA) was installed above the 2-D array to excite the red fluorescent paint.

To encourage crawling, animals were lined up on a linear elevated wooden substrate (standby track) leading to the force beam array. Caterpillars were found to move forward when naturally probed by another conspecific. On the 1-D beam array, data logging was started when the animal entered the buffer zone and stopped when either the animal stopped crawling or had covered the entire force bean array. For the shorter 2-D array, data logging did not begin until the thoracic legs triggered one of the active beams. After each trial, the animal was put back into the conditioning chamber for at least 3 min before it was returned to the standby track for another trial. All the data presented in this paper were from *Manduca* crawling horizontally in a straight-line, thus the normal GRFs (nGRFs) represent the body weight loading. A successful recording was one in which the caterpillar traveled *continuously* over the entire sensing zone. Since *Manduca* caterpillars tend to pause unpredictably, most animals produced only one successful trial during the experimental session. To be consistent, we analyzed only one successful trial from each of the eight experimental animals, resulting in five sets of nGRF data and three sets of 2-D (nGRF and fGRF) data.

Data processing

Because the caterpillars moved slowly, force data were sampled at 100 Hz, kinematics image analysis at 10 Hz, and behavioral videos at 30 frames per second. In preliminary experiments (nGRF recorded

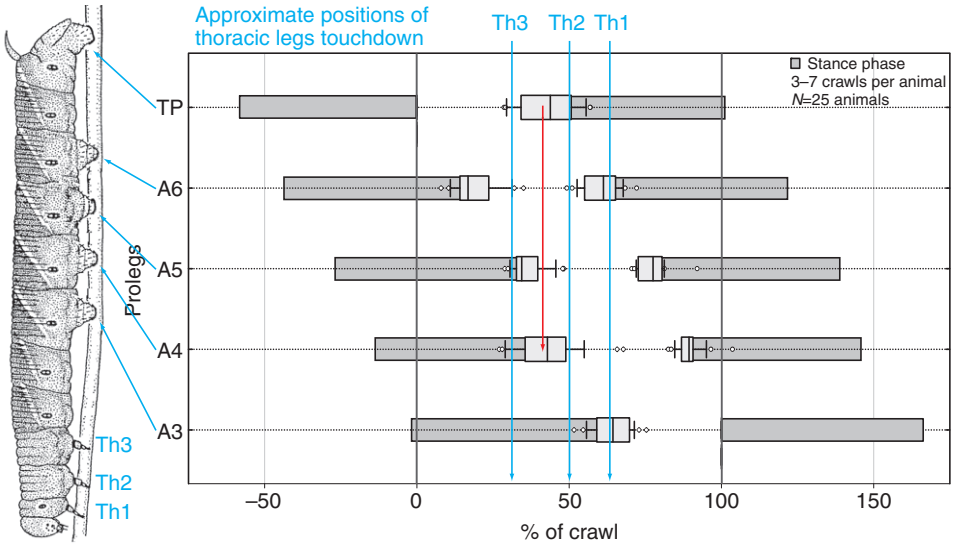

Fig. 2. *Manduca* standard kinematics template (SKT) and approximate thoracic legs touchdown. The relative timing of the stance and swing phases of each proleg during a crawl. The stance phase is shown as a grey bar with box plots marking the mean and 95% confidence intervals for the onset and end of stance [*N*=25 caterpillars; adapted from previously published data (van Griethuijsen and Trimmer, 2009)]. A complete crawl cycle (100%) was defined as the start of TP swing phase to the end of A3 stance phase (black vertical lines), corresponding to the TP takeoff and A3 touchdown of the next cycle. Notice that the TP touchdown tends to coincide with the A5 and A4 take-off (red arrow). The thoracic legs were not tracked during previous kinematic studies, so the approximate touchdown timing is based on video observations.

at 1 kHz) it was found that stepping forces changed over about 0.5 s and that most high frequency signals were due to electromagnetic noise. Occasional drift due to thermal fluctuation was too slow to interfere with the force recordings. The raw data was filtered using an RC type low-pass filter at 2 Hz and then smoothed with a second order polynomial over every 0.1 s. These curves were compared with the raw data to check consistency for every recording. Signal offsets were controlled under 6 mV and subtracted out using the reference recording. Raw voltages were converted to forces using calibration curves made for each beam.

The resulting GRF data were normalized to the individual caterpillar body weight (BW). The normalized data were then checked with the behavioral videos for single steps that occasionally occurred across two adjacent force beams and these readings were summed. Crawls with several such overlapping steps were rated as unsuccessful and removed from the analysis.

Force attribution

Video tracking provided the first indication of proleg touchdown timing and location. Individual proleg GRFs were then extracted by identifying the points at which stance occurred and by using threshold detection (normal load crosses 1% of the animal's body mass). The 2-D array captured at least one step per proleg in each trial. We therefore compiled at least one complete crawl cycle for each experimental animal for qualitative comparison. Although contact by a single pair of thoracic legs on the 2-D force beam was rare, some occurrences were identified from the videos. Examples of these 2-D GRFs have been included for comparison with the proleg GRFs.

Manduca standard kinematics template

Using the extensive kinematics data collected from our research group (von Griethuijsen and Trimmer, 2009; Trimmer and Issberner, 2007), the 2-D GRF data was scaled to the *Manduca* standard kinematics template representing the average step length and relative timing of proleg movements during a full crawl cycle (Fig. 2). The timing of the thoracic leg contacts are also noted on this template. A crawl cycle was defined as from the beginning of terminal prolegs swing phase to the beginning of A3 stance phase. We took the average stance phase time over a complete crawl time as the duty cycle of that particular proleg. By scaling all the corresponding GRF data to this template, we could analyze force interactions between different prolegs for different crawl cycles and animals. To match up thoracic legs in a crawl cycle, we analyzed the videos frame by frame to place the GRF data of the sample thoracic legs into the appropriated time points of a crawl cycle (as indicated in Fig. 2).

Weight shift analysis

Manduca caterpillars do not change length more than 5% during normal locomotion, so we could evaluate the overall weight shift by summing nGRFs from all contacts (including those from thoracic legs). This procedure produced an oscillating trace with each oscillation corresponding to one crawl cycle. Because inertial forces were so small these oscillations directly reflected the weight placements of the caterpillar. By measuring the loading change over each cycle, we could estimate how much mass was shifted forward and backward in one average step length (8.52 mm) per cycle period. Instead of tracking the center of mass, we assumed that only part of the body was accelerated forward in each crawl and that mechanical work associated with this weight shift could be evaluated.

RESULTS

Prolegs normal loading

During a crawl, a sequence of ground reaction forces was detected on each of the sensor beams. Frame-by frame analysis of the synchronized video allowed these forces to be attributed to different segmental appendages (Fig. 3A). Although the features of these forces varied in magnitude and duration each crawl, there were consistent differences in the nGRF profiles of each segment (Fig. 3B).

For the mid body segments (A4–A6) the ground impact and leg detachment were visible as two peaks in the nGRF data which overshot the weight-baring portion of the proleg stance phase. Behavioral observations suggested that these two peaks correspond to crochet protraction and retraction; both attachment and detachment involved momentary extension of the prolegs before the crochets grip or release. This may explain why there was no negative normal load in the recording of horizontal crawling. The initial loading and unloading rates were similar for each proleg in segments A3–A6 but differed for the terminal prolegs (TPs). After a more gradual loading phase, the TPs

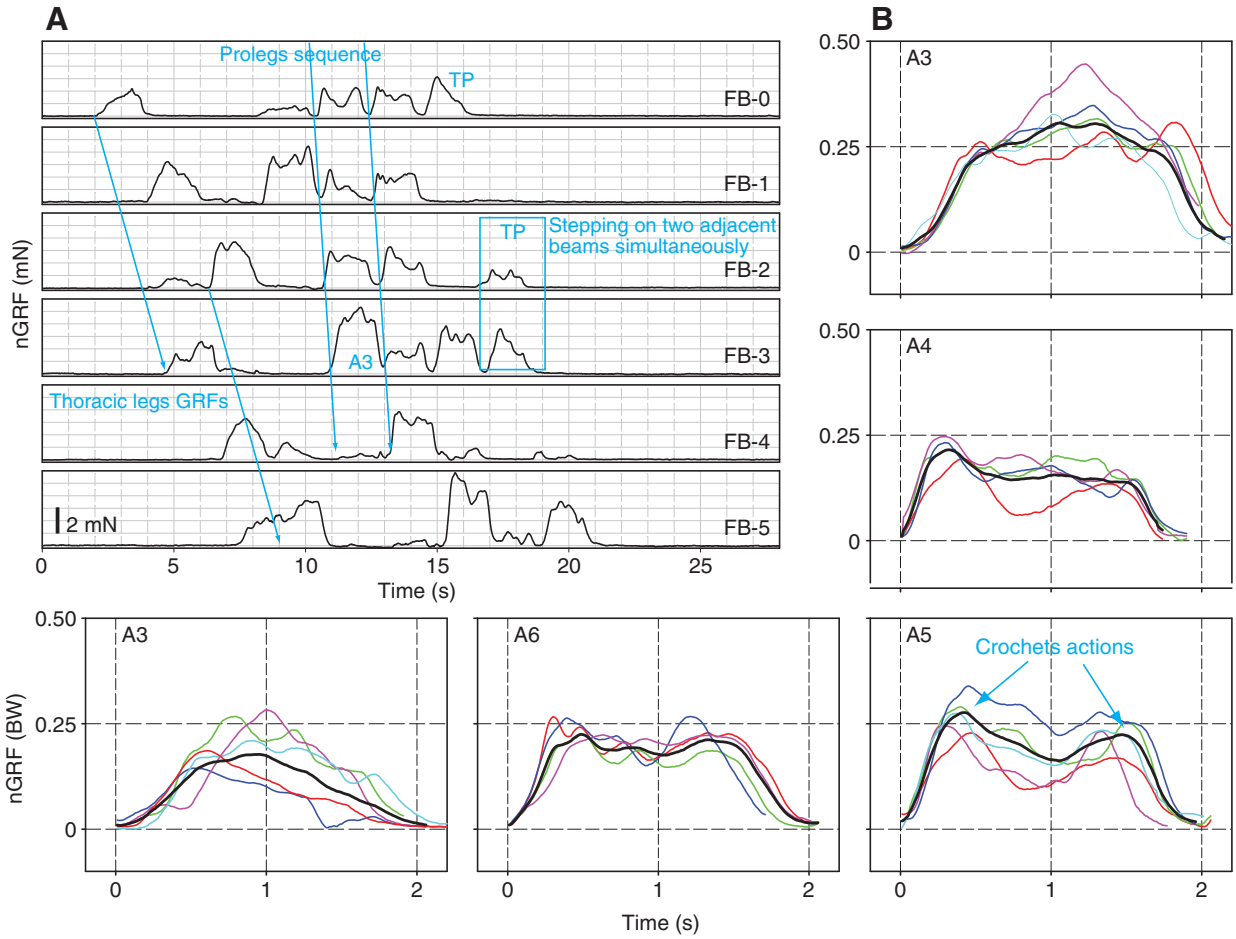

Fig. 3. *Manduca* normal GRFs representative data set. (A) Examples of the forces recorded simultaneously on six adjacent force beams (FB-0 to -5) during a crawl. Forces were recorded as the animal initially stepped onto FB-0 with its thoracic legs and then progressively moved across the beams until all of the proleg contact points were represented within the array. The final force profile in a sequence on each beam was that produced by the TP. In some instances (shown here on FB-2 and -3) the prolegs were in contact with two sensor beams simultaneously. Notice that each pair of prolegs generally loaded up to 25% of total body weight and thoracic legs took similar if not more weight at the front. Indeed, *Manduca* needs three or four minimum leg contacts at any given moment. (B) The nGRF profiles from each proleg can be extracted and overlaid with one another on successive steps (thin colored lines). The mean profile for these steps is then calculated and plotted as a thick dark line. The force profiles for prolegs A4–6 are often quite similar with peaks at the start and end of stance corresponding to the deployment and detachment of the crochets (arrows). The force profiles of proleg A3 and TP were variable but usually distinguishable from the mid-body segments with a mid-stance peak and different rates of onset and liftoff forces. See text for details.

immediately started to unload as the animal shifted its weight forward. The vertical reaction forces due to crochets were less pronounced for the TPs, but the weight-supporting section appeared highly variable just like the A3.

Weight shift

Overall weight shift can be observed from the net nGRF across all force beam channels. As the animal entered the sensor zone, forward and backward weight shifts appeared as nGRF fluctuation in each crawl cycle (Fig. 4A). When the animal was completely supported in the sensor zone the net nGRF was stable and equivalent to the weight of the animal (e.g. for Fig. 4 the average nGRF=16.94 mN, animal mass=1.72±0.01 g, or weight 16.9 mN). The 1-D array was accurate to within 10 µN for most recordings.

Although complete tracking of the center of mass throughout a crawl required a force beam array longer than the current device (one body length plus two additional steps), it was possible to perform a preliminary assessment of the overall weight shift during each step. The peak-to-peak net nGRF changes were measured for about 10 steps in each of five animals, standardized to the crawl cycle and body mass, and combined to show the overall weight shift in a crawl (Fig. 4B). During the first 64.5% of a step, *Manduca* shifted 30% of its body mass forward and then sharply arrested the transfer. Then it moved 15% of body mass back again in the last 35.5% of the step.

A brief note on thoracic legs

Although the sensor array was optimized for proleg reaction forces it was occasionally possible to detect GRFs from the thoracic legs collectively (Fig. 3) or segmentally (Fig. 5). From this sparse data it was observed that: (1) in all the thoracic GRF fragments, fGRF is almost always positive; (2) the nGRF results suggest that each thoracic leg supports as much body weight as each proleg; (3) force profiles for each thoracic leg overlap for much of the crawl cycle. Although the stiff articulated thoracic legs could withstand compressive forces they showed no indication of decelerating fGRFs (Fig. 5A), which suggests that the posterior segments do not push the thorax while it is in

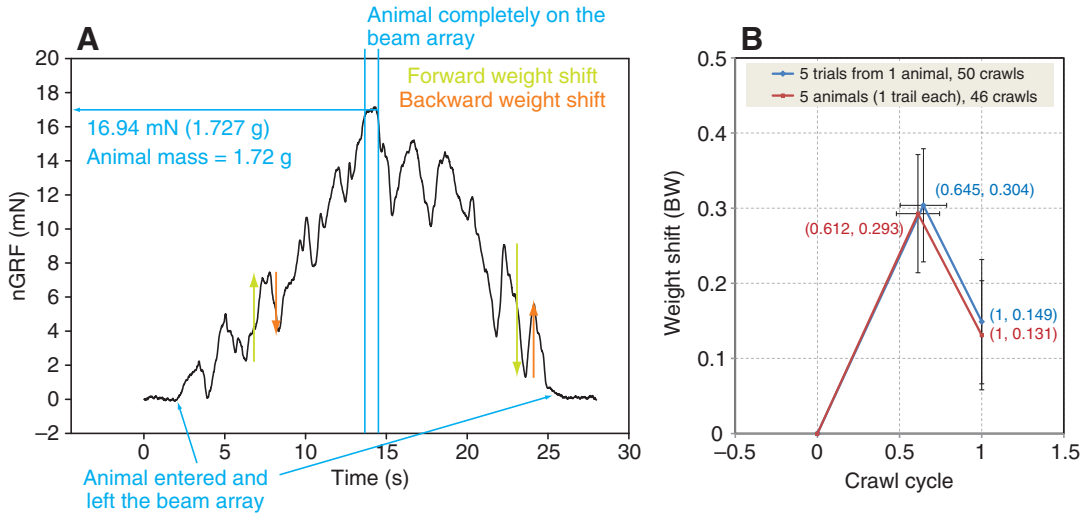

Fig. 4. *Manduca* weight shift analysis. (A) A representative recording of the net nGRF oscillations caused by weight shifts as *Manduca* moved across the sensor array. For about one second, the animal stood completely on the beam array and the net nGRF corresponded to the animal body weight (horizontal line on the top left). Weight shifts were quantified by measuring the peak-to-peak forward and backward changes as marked in green and orange, respectively. (B) These weight shifts (about 10 steps per trial) were measured in multiple trials from one animal (blue), and for one trial from each of five animals (red) and plotted as the mean proportion of body weight (BW) moving in each direction (± standard deviation, standard errors were negligibly small). *Manduca* shifted ~0.3 BW forward in the first ~0.65 of the crawl cycle before dropping ~0.15 BW back at the end of the crawl (as shown by the labeled coordinates). This resulted in a net weight transport of 0.15 BW per crawl, matching the observation of six or seven crawls per body length of travel. This oscillating mass shift predicts higher transient accelerations than those estimated from the kinematics and can be used to estimate the baseline mechanical energy associated with crawling locomotion. The body length of *Manduca* changed within 5% during normal locomotion (see Fig. 5B). Extra weight shift may contribute to large local deformation and internal mass redistribution.

stance. The timing of the thoracic maximum pull also coincides with periods of proleg 'drag' and this is presumably responsible for body stretching (at least from T1–A3) during locomotion. There is some redundancy in the mechanism of body extension since abdomen extension (A3–A10) can be achieved using proleg interactions alone although it may be less effective. Further examination of this unexpected role for the thoracic legs will require modification to the senor array in future studies.

Prolegs fore–aft loading

The reaction forces in the direction of locomotion (fGRF) are almost one magnitude higher than the normal loads (Fig. 5A). There are typically two negative impulses (decelerating forces) one at the start of stance and the other before the onset of swing, associated with proleg attachment and detachment. Terminal prolegs initiate each cycle with a decelerating impact and then rock briefly into a neutral state at about 20% of the stance phase. They then drag (negative fGRF) for most of the stance phase. A6 prolegs also decelerate during the terminal prolegs dragging phase, but they pivot into a positive pull as the terminal prolegs release from the substrate. Successive prolegs in segments A5–A3 share this force profile but the magnitude of the mid-stance fGRF is progressively less negative in more anterior segments and is generally positive (i.e. a pulling force) in segments A4 and A3.

For analytical purposes, we divided a complete crawl into two stages and six phases (Fig. 5B) as follows.

Stage (1) – abdominal contraction

Phase A [TP takeoff ~ A6 takeoff]

In the beginning of a crawl cycle, anterior prolegs are detached and pulled forward. At the same time, the thoracic legs starts to walk the thorax forward, stretching the frontal abdomen in the process (preliminary GRF data for thoracic legs). This initiates the overall mass shift.

Phase B [A6 takeoff ~ A5 takeoff]

The release of A6 immediately leads to more drag on the A5, indicating that the body tension anterior to A5 is initially higher than that between A6 and A5. This is also when the caterpillar reaches the shortest body length.

Phase C [A5 takeoff ~ A4 takeoff]

With the detachment of A5, the nGRF in A4 declines and that in A3 increases. This demonstrates that *Manduca* can lift its abdomen with only the A3 proleg and thoracic legs attached. Thoracic legs begin a new crawl cycle during this phase.

Stage (2) – abdominal stretching

Phase D [TP touchdown – A3 takeoff]

A4 detachment releases the muscle strain energy between A3 and A4, but this contraction is soon anchored by the TP. This initiates the stretching stage where anterior muscles stretch the posterior muscles between two bridging anchors.

Phase E [A6 touchdown – A5 touchdown]

A6 attaches to the substrate to hold the stretch and propagates this antagonist stretching forward. By now the caterpillar has returned to the original length, using the thoracic legs to maintain it. Body mass starts to rebound backward, probably through movements of internal organs and fluid.

Phase F [A5 touchdown – A3 touchdown]

The last phase of a crawl involves stretching the anterior abdomen back to its resting length using the thorax. Most abdominal muscles must do negative work in the process.

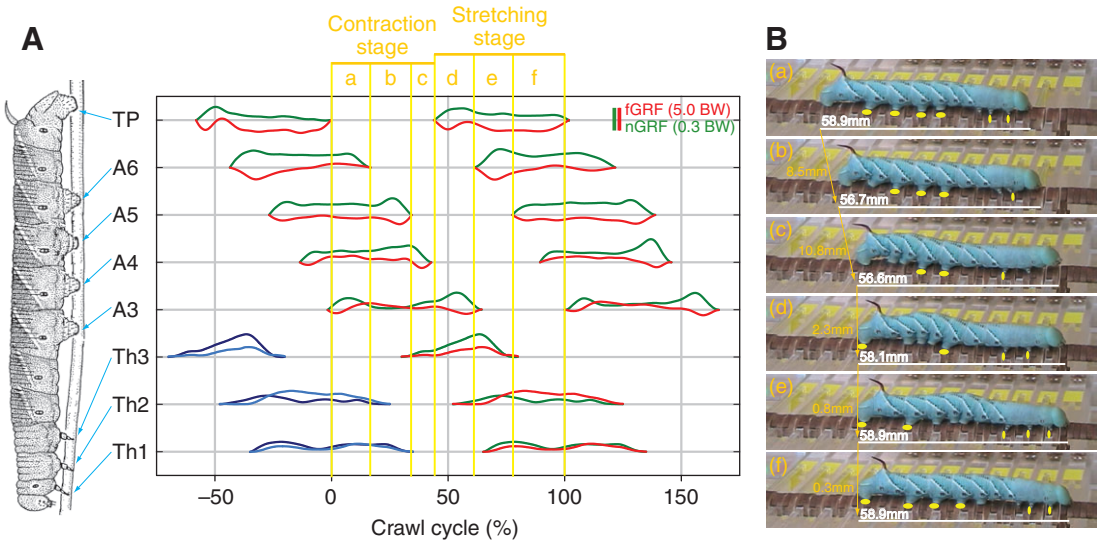

Fig. 5. Representative data of *Manduca* normal and fore–aft GRFs. (A) Examples of simultaneous recording of nGRF (in green) and fGRF (in red) scaled to the *Manduca* standard kinematics template (Fig. 2) to illustrate the overall timing of each proleg during a crawl cycle. This experiment was not designed to collect thoracic leg GRFs and thoracic legs were not tracked. However, for analytical purposes, one typical recording and its duplication (in blues) are manually inserted in this figure according to the behavioral videos. These data are representative of results from three experimental animals. All GRF traces are plotted as body weight (BW) as indicated by the reference bars on the upper right corner. Note that fGRF (scale bar is 5 BW) is much larger than nGRF (scale bar 0.3 BW). Indeed, nGRFs can be characterized by pure weight placement. (B) Six phases were identified in a crawl cycle. In the first stage (phases a–c) there was a progressive loss of contact points as the prolegs were lifted and the posterior part of the body shortened (up to 4–5% of original body length). Body tension anterior to the anchoring legs may be important in lifting the abdomen as the thorax extends during this contraction stage. In the subsequent stretching stage (phase d–f) the abdomen was stretched out by anchoring the anterior part of the body. The white bar in each snapshot reflects the caterpillar's current body length. The orange arrows indicate forward displacements of the body mid-point. A *Manduca* fifth instar caterpillar covered 33–45% of body length in each crawl. This sequence of movements can be used with the GRFs to predict muscle activation patterns and their associated work cycles (both negative and positive) (Dorfmann et al., 2008).

DISCUSSION

Prolegs = attachments

From detailed observations (Snodgrass, 1961) and kinematic analyses (Belanger and Trimmer, 2000; Mezoff et al., 2004; Trimmer and Issberner, 2007; van Griethuijsen and Trimmer, 2009) we proposed that caterpillars such as *Manduca* do not use the prolegs as actuated propulsive limbs, but instead use them as support and to generate controllable grip. For the first time it has now been possible to measure the GRFs during *Manduca* crawling and to show that the prolegs are indeed anchors rather than levers. An analysis of the GRF profiles and segmental timing reveals several new and unexpected details.

Stiff legs push, soft legs pull

Most vertebrates exploit their stiff skeleton and joints to transfer muscle forces directly into limb displacements. They can apply large compressive forces to the skeleton and typically use their hind legs to push off and the front legs to decelerate (Biewener, 2003). In contrast, the caterpillar prolegs are pouches of soft cuticle on the abdomen with no discrete articulation or structures for gaining a lever advantage. Moreover, because stress (and indirectly, stiffness) in the body wall is largely a function of hydrostatic pressure and curvature (Mezoff et al., 2004; Wainwright, 1988), it is impossible for the small radius prolegs to be stiffer than the body itself without additional chitin cross-linking or other structural changes. This means that prolegs are relatively soft and unsuitable for resisting large compressive loads. This is borne out by the fGRF results in which caterpillars mostly load their prolegs in tension and only momentarily experience compressive fGRF when TP and A6 'rock' the body mass over them. Caterpillars use the anterior prolegs to pull and the posterior prolegs to drag, effectively reversing the roles seen in most legged animals (Fanchon et al., 2006; Schmidt, 2005). Although the nGRFs during horizontal crawling are positive and therefore compress the prolegs (weight-bearing), these forces are an order of magnitude smaller than fGRFs and easily supported by baseline body pressure.

The role of a stiff substrate

It is clear from the fGRFs that the substrate takes the compressive load during multi-legged stance phases. This was verified using a simple behavioral test. *Manduca* was suspended from the head capsule and the dorsal horn and curved substrates of different stiffness but similar curvature (caterpillars prefer rode-like substrates) were placed between the prolegs as the caterpillar tried to crawl. As expected, relatively stiff substrates such as balsa wood were translocated backwards by the anterograde segment movements. However, as the substrate became softer these movements were less effective. When presented with a soft wire or a silk braid that could only take tensile loads, *Manduca* was unable to extend and its locomotory movements failed to move the wire progressively (Fig. 6). The substrate is therefore an essential component of this mechanical system, and *Manduca* is incapable of normal locomotion on surfaces that are softer and more compliant than its own body. Presumably, body stiffness is tunable within a narrow range through changes in muscle tone and internal pressure. This aspect of caterpillar locomotion could play an interesting ecological role since plant stiffness will affect the mobility of different caterpillar species. Unfortunately, we are not aware of any data correlating host plant foliage flexural stiffness to the mechanics of caterpillars feeding on them. We are therefore developing a numerical model of caterpillar mechanics based on tissue

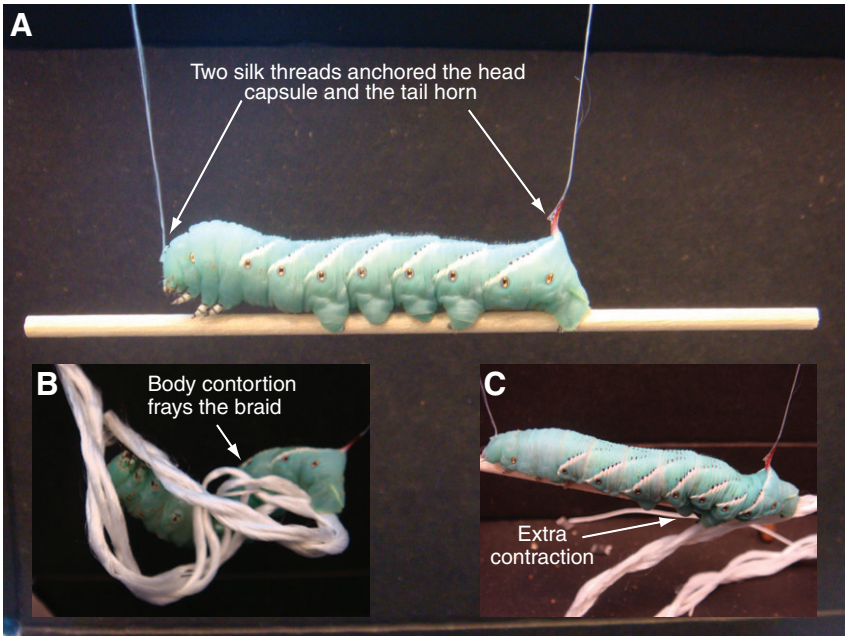

Fig. 6. The importance of substrate stiffness can be shown in a behavioral experiment. (A) A fifth instar caterpillar was suspended from its head capsule and the dorsal horn but was otherwise free to move. It demonstrated normal crawling movements when a light piece of stiff balsa wood was placed between the prolegs. The wood steadily moved backwards as *Manduca* attempted to make forward progress. (B) When *Manduca* was presented with materials that deformed under compressive loads it was unable to extend its body or maintain a normal posture. For example, when a *Manduca* caterpillar tried to crawl on a silk braid (the same diameter as the balsa wood stick) the body became curved and it could not extend the anterior segments to make forward progress. Eventually, it started to fray the silk braid by pullling threads together. (C) When the entangled caterpillar was then allowed to move onto the balsa wood substrate it recovered normal crawling as the prolegs gradually reached the stiff substrate. Notice the extra body contraction at the interface between the silk braid and the balsa stick. The abdominal segments regained normal length only when their associated prolegs attached to the stiffer substrate.

material properties (Lin et al., 2009), morphology and pressure (H.T.L., unpublished data). We intend to check this model against some ecological and morphological data in the near future.

Statics? Dynamics?

The weight shift estimation (Fig. 4) allows us to calculate the real locomotor acceleration and its associated forces for a fifth instar *Manduca* crawling with a single step length of 8.52 mm. According to the weight shift estimate, a 2.50 g caterpillar would move 0.3 of body weight (BW) in 0.654 of a crawl cycle. We can calculate the time for this forward weight shift from the average crawl period 2.778 s (t=2.778 s×0.654=1.817 s). Assuming constant acceleration and that the mass moves with negligible friction, we can write:

$$\mathbf{a} = \frac{d}{t^2} = \frac{8.52(\text{mm})}{1.817^2(\text{s}^2)} = 2.58\left(\frac{\text{mm}}{\text{s}^2}\right), \quad (1)$$

where **a** is acceleration, d is step length, t is time; and

$$\mathbf{F} = m\mathbf{a} = 2.5(\text{g}) \times 0.3(\text{BW}) \times 2.58\left(\frac{\text{mm}}{\text{s}^2}\right) = 1.94(\mu\text{N}), \quad (2)$$

where **F** is the accelerating force, and m is the body mass. This is a very small force (the single leg vertical force from a running *Blaberus* cockroach of similar weight peaks at 17 mN and the horizontal force is 5 mN (Full et al., 1995). With more funding and instrumentation, it is possible to expand the 2-D force beam array to cover all the *Manduca* contact points simultaneously and directly demonstrate that the sum of the fGRFs is effectively zero.

Based on this force estimate, we can calculate the minimum energy expense associated with weight shift. Since the caterpillar prolegs have no leverage, we assume the breaking impulse provided by soft-tissues and the backward weight shift to be passive rebound. The energy expenditure (E) is therefore only in the forward mass acceleration:

$$E = \mathbf{F}d = 1.94(\mu\text{N}) \times 8.52(\text{mm}) \approx 16.5 \times \text{nJ} \quad (3)$$

and locomotor power (P) over a crawl period (T):

$$P = \frac{E}{T} = \frac{16.5(\text{nJ})}{2.778(\text{s})} \approx 5.94 \times \text{nW}. \quad (4)$$

This tiny energy expenditure per crawl can be converted to the cost of transport per kilogram of body mass: $E/2.5(\text{g})=6.6\times10^{-6}\,\text{J kg}^{-1}$. It is indeed an insignificant fraction of the average cost of transport of either a gypsy moth caterpillar ($3.6\,\text{J kg}^{-1}$) (Casey, 1991) or a *Manduca* caterpillar ($22.5\,\text{J kg}^{-1}$, N=5; W. Woods, Jr, personal communication). Caterpillar locomotion involves shortening and lengthening low resilience tissues (Lin et al., 2009) and viscous hemolymph, which all dissipate energy. In short, the energy required to move the body mass forward is minuscule because of the static nature of the locomotion. Most energy exchange is mediated by tissue stretching and recoil, further emphasizing the importance of pseudo- and visco-elastic properties of the tissues themselves.

Antagonist stretching and efficiency

Although *Manduca* is capable of extending its body using hydrostatic turgor (e.g. exploratory reaching/casting behavior) during horizontal crawling on a (relatively) stiff substrate, it instead uses the substrate to stretch out. In this process, the thorax walks forward but does not bring the heavy abdomen with it, thereby stretching the anterior segments. Abdominal segments shorten partly by releasing muscle strain energy between adjacent prolegs. To stretch the abdomen back out, the caterpillar anchors its two ends and pulls the posterior muscles with anterior muscles. Forces in the axial direction are responsible for extending the body and restoring muscle length which explains why fGRFs are much larger than the nGRFs. This is similar to the antagonist muscle stretching in vertebrates or stiff skeleton arthropods and it may convey several biomechanical advantages over a hydrostatic skeleton. First, by using the substrate as a skeleton, *Manduca* avoids the need to strongly pressurize its fluid filled body; the body can be just stiff enough for self support. Second, by conforming to the substrate directly there is no need to maintain posture through local pressure control; the body does not need to be compartmentalized and the demands for neural-computation and proprioception can be minimized. Third, by avoiding hydrostatic control of locomotion, internal organ systems that interface with the exterior (e.g. gas exchange and digestion) can be decoupled from movements (in contrast to the hydrostatic limb extension system of many spiders that makes fast running and breathing incompatible (Parry and Brown, 1959; Prestwich, 1988). These physiological

advantages could also be evolutionary constraints that have contributed to the unique locomotion of caterpillars in general.

Implications on caterpillar prolegs diversity

From lepidopteron homeotic gene studies (Suzuki and Palopoli, 2001; Warren et al., 1994), comparative anatomy (Hinton, 1955) and X-ray induced mutation (M. A. Simon, personal communication), we know that caterpillars are capable of generating prolegs in any abdominal segments. It is therefore interesting that some caterpillars share the same body plans whereas others differ so much. The new findings on caterpillar GRFs may provide insights into some of the biomechanical constraints favoring the evolution of different proleg configurations.

According to the GRF analysis in this study, prolegs anchor a caterpillar for body deformation. The posterior legs are responsible for holding the rear end while the anterior muscles stretch the abdominal muscles. During this process, the substrate takes on compressive loads and transmits the necessary forces across the body, analogous to a rigid bone in a skeletal system. This strategy is methodologically different from that of hydrostatic and articulated skeletons. Since the animal does not carry its own skeleton and simply adopts whatever it sits on, we call it an 'environmental skeleton'. In a typical caterpillar body plan, the lack of prolegs in A7–A9 provides clearance for the terminal prolegs (TP) to swing forward and thus limits of the step size. *Manduca*'s center of mass is in A4, so the adjacent prolegs A3–A5 are critical for securing the body. Species that have a reduced number of prolegs in these segments may have an increased dependence on a hydrostatic skeleton. For example, we predict that caterpillars with looping gaits (and few proleg attachments) will have biomechanics dominated by a hydrostatic skeleton. However, in both *Manduca* casting behavior and inchworm looping locomotion, the A6 prolegs work closely with the terminal prolegs to produce leverage *via* the hydrostatic skeleton.

It is interesting to speculate on the evolutionary transition from ancestral crawling that relies so much on the substrate, to looping gaits. Since the cost of maintaining a hydrostatic skeleton is determined by the pressure required to inflate the body it is conceivable that as the caterpillars adapted to narrower environmental niches, their body size decreased and body stiffness increased. Under these conditions, the use of a hydrostatic skeleton may be more favorable than the environmental skeleton. The findings reported here provide a new basis for exploring the relatively neglected role of locomotory mechanics in the evolutionary ecology of plant–insect interactions.

ACKNOWLEDGEMENTS

We would like to thank Caroline Blavet for collecting some nGRF data and Linnea van Griethuijsen for providing assistance in constructing the *Manduca* standard kinematics template. The *Manduca* cost of transport data was provided by Dr William Woods. This project was funded by NSF grant IOS 0718537 to B.A.T.

REFERENCES

Barth, R. (1937). Muskulatur Und Bewegungsart Der Raupen. *Zool. Jb. Physiol.* **62**, 507-566.
Bartsch, M. S., Federle, W., Robert, J. and Kenny, T. W. (2007). A multiaxis force sensor for the study of insect biomechanics. *J. Microelectromech. Syst.* **16**, 709.
Belanger, J. H. and Trimmer, B. A. (2000). Combined kinematic and electromyographic analyses of proleg function during crawling by the caterpillar *Manduca Sexta*. *J. Comp. Physiol. A* **186**, 1031-1039.
Belanger, J. H., Bender, K. J. and Trimmer, B. A. (2000). Context dependency of a limb withdrawal reflex in the caterpillar *Manduca Sexta*. *J. Comp. Physiol. A* **186**, 1041-1048.
Bell, R. A. and Joachim, F. G. (1976). Techniques for rearing laboratory colonies of tobacco hornworms and pink bollworms. *Ann. Entomol. Soc. Am.* **69**, 365-373.
Biewener, A. A. (2003). *Animal Locomotion.* Oxford University Press, USA.
Blickhan, R., Seyfarth, A., Geyer, H., Grimmer, S., Wagner, H. and Günther, M. (2007). Intelligence by mechanics. *Phil. Trans. R Soc. Lond. A* **365**, 199-220.
Casey, T. M. (1991). *Energetics of caterpillar locomotion: biomechanical constraints of a hydraulic skeleton. Science* **252**, 112-114.
Chapman, G. (1958). The hydrostatic skeleton in the invertebrates. *Biol. Rev.* **33**, 338-371.
Chiel, H. J., Crago, P., Mansour, J. M. and Hathi, K. (1992). Biomechanics of a muscular hydrostat: a model of lapping by a reptilian tongue. *Biol. Cybern.* **67**, 403-415.
Colobert, B., Crétual, A., Allard, P. and Delamarche, P. (2006). Force-plate based computation of ankle and hip strategies from double-inverted pendulum model. *Clin. Biomech.* **21**, 427-434.
Dominick, O. S. and Truman, J. W. (1986). The physiology of wandering behaviour in *Manduca Sexta*. III. organization of wandering behaviour in the larval nervous system. *J. Exp. Biol.* **121**, 115-132.
Dorfmann, A., Trimmer, B. A. and Woods, W. A. (2008). Muscle performance in a soft-bodied terrestrial crawler: constitutive modeling of strain-rate dependency. *J. R. Soc. Interface* **5**, 349-362.
Dutto, D. J., Hoyt, D. F., Cogger, E. A. and Wickler, S. J. (2004). Ground reaction forces in horses trotting up an incline and on the level over a range of speeds. *J. Exp. Biol.* **207**, 3507-3514.
Eaton, J. L. (1988). *Lepidopteran Anatomy.* New York: Wiley.
Epstein, M. E. (1996). Revision and phylogeny of the limacodid group families, with evolutionary studies on slug caterpillars (Lepidoptera: Zygaenoidea). *Smithson Contrib. Zool.* **582**, 1-102.
Fanchon, L., Valette, J. P., Sanaa, M. and Grandjean, D. (2006). The measurement of ground reaction force in dogs trotting on a treadmill: an investigation of habituation. *Vet. Comp. Orthop. Traumatol.* **19**, 81-86.
Forbes, W. (1910). A structural study of some caterpillars. *Ann. Entomol. Soc. Am.* **3**, 94-143.
Full, R. J., Yamauchi, A. and Jindrich, D. L. (1995). Maximum single leg force production: cockroaches righting and running on photoelastic gelatin. *J. Exp. Biol.* **198**, 2441-2452.
Goldman, D. I., Chen, T. S. and Dudek, D. M. (2006). Dynamics of rapid vertical climbing in cockroaches reveals a template. *J. Exp. Biol.* **209**, 2990-3000.
Heglund, N. C. (1981). A simple design for a force-plate to measure ground reaction forces. *J. Exp. Biol.* **93**, 333-338.
Herrel, A., Meyers, J. J., Timmermans, J. P. and Nishikawa, K. C. (2002). Supercontracting muscle: producing tension over extreme muscle lengths. *J. Exp. Biol.* **205**, 2167-2173.
Hinton, H. E. (1955). On the structure, function, and distribution of the prolegs of the panorpoidea, with a criticism of the Berlese-Imms Theory. *Trans. R. Entomol. Soc. Lond.* **106**, 455-540.
Holmes, P., Robert, J., Koditschek, D. E. and Guckenheimer, J. (2006). The Dynamics of legged locomotion: models, analyses, and challenges. *SIAM Reviews* **48**, 207-304.
Johnston, R. M. and Levine, R. B. (1996a). Crawling motor patterns induced by pilocarpine in isolated larval nerve cords of *Manduca Sexta*. *J. Neurophysiol.* **76**, 3178-3195.
Johnston, R. M. and Levine, R. B. (1996b). Locomotory behavior in the hawkmoth *Manduca sexta*: kinematic and electromyographic analyses of the thoracic legs in larvae and adults. *J. Exp. Biol.* **199**, 759-774.
Keudel, M. and Schrader, S. (1999). Axial and radial pressure exerted by earthworms of different ecological groups. *Biol. Fertility Soils* **29**, 262-269.
Kier, W. M. (1992). Hydrostatic skeletons and muscular hydrostats. In *Biomechanics (Structures and Systems): A Practical Approach* (ed. A. A. Biewener), pp. 205-231. New York: IRL Press at Oxford University Press.
Kier, W. M. and Smith, K. K. (1985). Tongues, tentacles and trunks: the biomechanics of movement in muscular-hydrostats. *Zool. J. Linn. Soc.* **83**, 307-324.
Kier, W. M. and Stella, M. P. (2007). The arrangement and function of octopus arm musculature and connective tissue. *J. Morphol.* **268**, 831-843.
Kopec, S. (1919). Lokalizationsversuche an Zentralen Nervensysyteme Der Raupen Und Falter. *Zool. Jb. Physiol.* **36**, 453-502.
Kristan, W. B., Calabrese, R. L. and Friesen, W. O. (2005). Neuronal control of leech behavior. *Prog. Neurobiol.* **76**, 279-327.
Lemmerhirt, D. F., Staudacher, E. M. and Wise, K. D. (2006). A Multitransducer microsystem for insect monitoring and control. *IEEE Trans. Biomed. Eng.* **53**, 2084-2091.
Levine, R. B. and Truman, J. W. (1985). Dendritic reorganization of abdominal motoneurons during metamorphosis of the moth, Manduca Sexta. *J. Neurosci.* **5**, 2424-2431.
Libby, J. L. (1959). The Nervous system of certain abdominal segments of the *Cecropia larva* (Lepidoptera: Saturniidae). *Ann. Entomol. Soc. Am.* **52**, 469-480.
Lin, H. T., Dorfmann, A. L. and Trimmer, B. A. (2009). Soft-cuticle biomechanics: a constitutive model of anisotropy for caterpillar integument. *J. Theor. Biol.* **256**, 447-457.
McKenzie, B. M. and Dexter, A. R. (1988a). Axial pressures generated by the earthworm *Aporrectodea Rosea*. *Biol. Fertility Soils* **5**, 323-327.
McKenzie, B. M. and Dexter, A. R. (1988b). Radial pressures generated by the earthworm *Aporrectodea Rosea*. *Biol. Fertility Soils* **5**, 328-332.
Mezoff, S., Papastathis, N., Takesian, A. and Trimmer, B. A. (2004). The Biomechanical and neural control of hydrostatic limb movements in *Manduca Sexta*. *J. Exp. Biol.* **207**, 3043-3053.
Miller, J. C., Janzen, D. H. and Hallwachs, W. (2006). *100 Caterpillars*. Cambridge, MA: Belknap Press of Harvard University Press.
Niebur, E. and Erdos, P. (1991). Theory of the locomotion of nematodes: dynamics of undulatory progression on a surface. *Biophys. J.* **60**, 1132.
Nishikawa, K. C., Kier, W. M. and Smith, K. K. (1999). Morphology and mechanics of tongue movement in the african pig-nosed frog *Hemisus Marmoratum*: a muscular hydrostatic model. *J. Exp. Biol.* **202**, 771-780.
Parry, D. A. and Brown, R. H. J. (1959). The hydraulic mechanism of the spider leg. *J. Exp. Biol.* **36**, 423-433.
Prestwich, K. N. (1988). The constraints on maximal activity in spiders. *J. Comp. Physiol. B* **158**, 437-447.

Quillin, K. J. (1998). Ontogenetic scaling of hydrostatic skeletons: geometric, static stress and dynamic stress scaling of the earthworm *Lumbricus terrestris*. *J. Exp. Biol.* **201**, 1871-1883.
Quillin, K. J. (1999). Kinematic scaling of locomotion by hydrostatic animals: ontogeny of peristaltic crawling by the earthworm*Lumbricus terrestris*. *J. Exp. Biol.* **202**, 661-674.
Quillin, K. J. (2000). Ontogenetic scaling of burrowing forces in the earthworm *Lumbricus terrestris*. *J. Exp. Biol.* **203**, 2757-2770.
Reinhardt, L., Weihmann, T. and Blickhan, R. (2009). Dynamics and kinematics of ant locomotion: do wood ants climb on level surfaces? *J. Exp. Biol.* **212**, 2426.
Roberts, T. J. and Belliveau, R. A. (2005). Sources of mechanical power for uphill running in humans. *J. Exp. Biol.* **208**, 1963-1970.
Rubinoff, D. and Haines, W. P. (2005). Web-spinning caterpillar stalks snails. *Science* **309**, 575.
Schmidt, M. (2005). Quadrupedal locomotion in squirrel monkeys (Cebidae: Saimiri Sciureus): A cineradiographic study of limb kinematics and related substrate reaction forces. *Primates* **128**, 359-370.
Simon, M. A. and Trimmer, B. A. (2009). Movement encoding by a stretch receptor in the soft-bodied caterpillar, *Manduca sexta*. *J. Exp. Biol.* **212**, 1021.
Skierczynski, B. A., Wilson, R. J. A., Kristan, W. B., Jr and Skalak, R. (1996). A model of the hydrostatic skeleton of the leech. *J. Theor. Biol.* **181**, 329-342.
Smolianinov, V. V. and Mazurov, M. E. (1976). Kinematics of crawling locomotion. I. Ideal elastic model. *Biofizika* **21**, 1103-1108.
Snodgrass, R. E. (1961). The caterpillar and the butterfly. Smithsonian Miscellaneous Collections 143, pp. 1–51. Washington, DC: Smithsonian Institution.
Snodgrass, R. E. (1993). *Principles of Insect Morphology*. Ithaca: Cornel University Press.
Suzuki, Y. and Palopoli, M. F. (2001). Evolution of insect abdominal appendages: are prolegs homologous or convergent traits? *Dev. Genes Evol.* **211**, 486-492.
Taylor, H. M. and Truman, J. W. (1974). Metamorphosis of the abdominal ganglia of the tobacco hornworm, *Manduca sexta*. *J. Comp. Physiol. A* **90**, 367-388.
Trimmer, B. A. and Issberner, J. (2007). Kinematics of soft-bodied, legged locomotion in *Manduca sexta* larvae. *Biol. Bull.* **212**, 130.
van Griethuijsen, L. I. and Trimmer, B. A. (2009). Kinematics of horizontal and vertical caterpillar crawling. *J. Exp. Biol.* **212**, 1455.
Wadepuhl, M. and Beyn, W. J. (1989). Computer simulation of the hydrostatic skeleton. The physical equivalent, mathematics and application to worm-like forms. *J. Theor. Biol.* **136**, 379-402.
Wagner, D. L. (2005). *Caterpillars of Eastern North America: A Guide to Identification and Natural History*: Princeton, NJ: Princeton University Press.
Wainwright, S. A. (1988). *Axis and Circumference: The Cylindrical Shape of Plants and Animals*. Cambridge: Harvard University Press.
Warren, R. W., Nagy, L., Selegue, J., Gates, J. and Carroll, S. (1994). Evolution of homeotic gene regulation and function in flies and butterflies. *Nature* **372**, 458-461.
Weeks, J. C. and Truman, J. W. (1984). Neural organization of peptide-activated ecdysis behaviors during the metamorphosis of *Manduca sexta*. *J. Comp. Physiol. A* **155**, 407-422.
Zumwalt, A. C., Hamrick, M. and Schmitt, D. (2006). Force plate for measuring the ground reaction forces in small animal locomotion. *J. Biomech.* **39**, 2877-2881